Int. J. Electrochem. Sci., 17 **(2022)** Article Number: 220621, doi: 10.20964/2022.06.40

International Journal of
ELECTROCHEMICAL
SCIENCE
www.electrochemsci.org

Short Communication

Effect of Different Corrosion Inhibitors on Corrosion of AM60B Magnesium Alloy in Simulated Vehicle Coolant

Binghao Shu[*], *Jiao Xue*

Henan Mechanical and Electrical Vocational College, Zhengzhou 451191, China
[*]E-mail: shubh_edu@126.com

Received: 6 February 2022 / *Accepted:* 19 March 2022 / *Published:* 7 May 2022

Sodium alginate, sodium silicate and sodium dodecyl benzene sulfonate were selected as the corrosion inhibitors, and the corrosion resistance of AM60B magnesium alloy in simulated vehicle coolant containing different corrosion inhibitors was investigated. The results show that using sodium alginate, sodium silicate or sodium dodecyl benzene sulfonate as corrosion inhibitor can inhibit the corrosion of AM60B magnesium alloy in simulated vehicle coolant to reduce corrosion rate. When sodium silicate is used as corrosion inhibitor, the corrosion current density of AM60B magnesium alloy decreases extremely compared with that without corrosion inhibitor, and the charge transfer resistance increases by nearly two times. The corrosion rate of AM60B magnesium alloy is the lowest when immersed in simulated vehicle coolant containing sodium silicate. Moreover, the corrosion inhibition efficiency of sodium silicate for AM60B magnesium alloy reaches 96%, which is better than sodium alginate and sodium dodecyl benzene sulfonate. Sodium silicate is considered as an ideal corrosion inhibitor which can effectively inhibit the corrosion of AM60B magnesium alloy in simulated vehicle coolant.

Keywords: Corrosion inhibition effect; AM60B magnesium alloy; Simulated vehicle coolant; Sodium alginate; Sodium silicate; Sodium dodecyl benzene sulfonate

1. INTRODUCTION

Magnesium alloy has the advantages of light weight, strong strength, good casting and size stability, which is an ideal material for manufacturing the vehicle engine cylinder block and its cooling system [1-5]. However, the electrode potential of the magnesium alloy is very low. Moreover, the surface of magnesium alloy is loose and porous that limits its protective effect. Therefore, the magnesium alloy is easily corroded in the acid and alkaline solution. Vehicle coolant is the medium used by the engine cooling system, which is composed of basic liquid, water and various additives. Because the vehicle engine cooling system is a very special environment, the dynamic change in temperature differential causes the corrosion of magnesium alloy in the coolant system. The corrosion

is from local corrosion to comprehensive corrosion, eventually resulting in premature failure of magnesium alloy structure [6-9]. Therefore, how to effectively inhibit the corrosion of magnesium alloy in the vehicle coolant system has become an urgent problem.

It was found out that adding suitable corrosion inhibitor can slow down the corrosion of magnesium alloy. Common corrosion inhibitor includes rare earth, tungstate, silicate, phosphate and so on. For example, rare earth not only can be added to the corrosion solution to play a role of corrosion inhibition, but also can be introduced in the process of preparing materials to improve the corrosion resistance of materials [10-14]. Moreover, tungstate is found to be a good corrosion inhibitor and an optimal doping material for metal alloys to improve corrosion resistance [15-22]. At present, some scholars have studied the corrosion inhibition effect of common corrosion inhibitors. However, most of the studies are only aimed at the corrosion inhibition effect of a single corrosion inhibitor. It is significant to investigate and compare different corrosion inhibitors on the corrosion inhibition effect. In this paper, sodium alginate, sodium silicate and sodium dodecyl benzene sulfonate (SDBS) were selected as the corrosion inhibitors. The electrochemical corrosion and immersion corrosion experiments were carried out in simulated vehicle coolant, and the corrosion inhibition of different corrosion inhibitors for magnesium alloy was compared. The corrosion resistance of AM60B magnesium alloy in simulated vehicle coolant containing different corrosion inhibitors was investigated to compare the corrosion inhibition effect. The aim is to find out an ideal corrosion inhibitor for AM60B magnesium alloy in simulated vehicle coolant.

2. EXPERIMENTAL

2.1 Pretreatment of AM60B magnesium alloy

The AM60B magnesium alloy plate (thickness is 3 mm) is chosen as the substrate, which is composed of Al 5.6%~6.4%, Mn 0.26%~0.5%, Zn 0.2%, Si 0.5%, surplus is Mg. The surface of the substrate is polished with 800 #, 1500 # and 2000 # sandpaper to ensure smoothness. And then, the substrate is cleaned in acetone solution for 5 min in ultrasonic environment to remove oil. Finally, it is washed with deionized water and dried.

2.2 Preparation of simulated vehicle coolant

According to the China's petrochemical industry standard SH/T 0085 “Test Method for Corrosion of Engine Coolant (Glassware Method)”, the ethylene glycol, sodium chloride, sodium sulfate, sodium bicarbonate and deionized water are combined to prepare 2000 mL of simulated vehicle coolant. The main composition is shown in Table 1. After stirring evenly, the simulated vehicle coolant was divided into four portions of 500 mL each, and placed in beakers marked S1, S2, S3, and S4 respectively. 20 mg/L sodium alginate is added to the beaker marked S1 while 110 mg/L sodium silicate was added to the beaker marked S2. Moreover, 600 mg/L SDBS was added to the beaker marked S3. As a control, no corrosion inhibitor was added to the beaker marked S4.

Table 1. Main composition of simulated vehicle coolant

Chemical agents	Concentration
ethylene glycol	500 mL/L
sodium chloride	135 mg/L
sodium sulfate	100 mg/L
sodium bicarbonate	150 mg/L

2.3 Testing and analysis

2.3.1 Polarization curves and electrochemical impedance spectrum

PARSTAT 2273 electrochemical workstation was used to test the polarization curve and electrochemical impedance spectrum respectively. AM60B magnesium alloy sample was the working electrode while platinum electrode was the auxiliary electrode, and saturated calomel electrode was the reference electrode. The electrodes were immersed in simulated vehicle coolant for one hour before testing to reach a steady state. A scanning rate of 1 mV/s was used for the polarization curve and the test data were analyzed using PowerSuite software to obtain the corrosion potential and corrosion current density. The AC signal amplitude applied by the electrochemical impedance spectrum test was 5 mV with a frequency range of 10^5 to 10^{-2} Hz, and the test data was analyzed using ZsimpWin software to obtain the charge transfer resistance.

The corrosion inhibition efficiency of different corrosion inhibitors on AM60B magnesium alloy in simulated vehicle coolant is calculated according to the following equation:

$$\eta = \frac{J_{corr} - J''_{corr}}{J_{corr}} \times 100\% \quad (1)$$

In the equation, η represents the corrosion inhibition efficiency. J_{corr} and J''_{corr} represent the corrosion current density of AM60B magnesium alloy in simulated vehicle coolant without corrosion inhibitor and with corrosion inhibitors, respectively, and the units are A/cm^2.

2.3.2 Corrosion rate

AM60B magnesium alloy samples with the same size (25 mm×12 mm×3 mm) were immersed in simulated vehicle coolant without corrosion inhibitor and with different corrosion inhibitors by suspension method for 15 d and 25 d, respectively. After the experiment, the corrosion products were removed, and then the sample was cleaned with deionized water and dried. The corrosion rate of AM60B magnesium alloy was calculated according to the following equation:

$$v_{corr} = \frac{m_{before} - m_{after}}{S \cdot t} \quad (2)$$

In equation, V_{corr} indicates the corrosion rate using the unit g/(m^2·d). m_{before} and m_{afte} indicate the quality before and after corrosion of AM60B magnesium alloy samples, unit is g. *S* indicates the sample surface area using the unit m^2 while *t* is the immersion time (d).

2.3.3 Surface morphology

SuperView W1 surface profilometer and Nova NanoSEM450 scanning electron microscope were used to observe the three-dimensional and microscopic morphology of AM60B magnesium alloy before and after corrosion in simulated vehicle coolant without corrosion inhibitor and with different corrosion inhibitors.

3. RESULT AND DISCUSSION

3.1 Analysis of polarization curves

Figure 1 shows the polarization curves of AM60B magnesium alloy in simulated vehicle coolant with and without corrosion inhibitors. The polarization curves of the AM60B magnesium alloy and some protection coatings prepared on AM60B magnesium alloy have been investigated in some papers [23-27]. Compared with the preparation of protection coating on magnesium alloy to improve the corrosion resistance of magnesium alloy, it is cheaper to add corrosion inhibitor into the corrosion solution to improve the corrosion resistance of magnesium alloy. As can be seen from Figure 1, with the addition of sodium alginate, sodium silicate or SDBS, the polarization curve of AM60B magnesium alloy shifts to the lower right and the corrosion current density is reduced compared to that without inhibitors. This indicates that sodium alginate, sodium silicate or SDBS can inhibit the corrosion process of magnesium alloy in simulated vehicle coolant to some extent.

As can be seen from Table 2, there are certain differences in corrosion potential and corrosion current density of AM60B magnesium alloy in simulated vehicle coolant with different corrosion inhibitors. Specifically, the corrosion current density of AM60B magnesium alloy with sodium alginate as corrosion inhibitor is less than one order of magnitude lower than that without corrosion inhibitor. Compared with simulated vehicle coolant without corrosion inhibitor, the corrosion current density of AM60B magnesium alloy with sodium silicate or SDBS as corrosion inhibitor decreases by more than one order of magnitude to 12.4 μA/cm^2 and 25.6 μA/cm^2, respectively. It is concluded that sodium silicate has the best corrosion inhibition effect on the corrosion process of AM60B magnesium alloy, and it can more effectively inhibit the corrosion of AM60B magnesium alloy in simulated vehicle coolant.

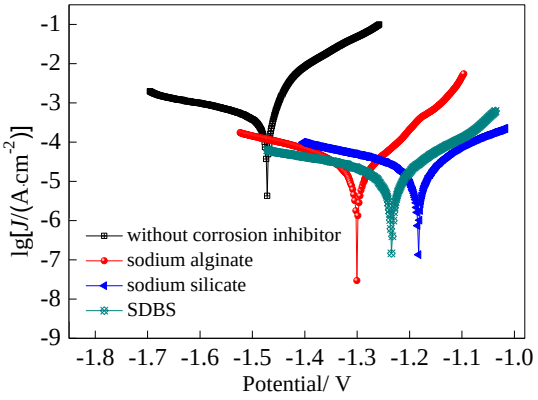

Figure 1. Polarization curves of AM60B magnesium alloy in simulated vehicle coolant with and without corrosion inhibitors

Table 2. Corrosion potential and corrosion current density of polarization curves

Different corrosion inhibitors	Corrosion potential/ V	Corrosion current density/ (A·cm^{-2})	Anode Tafel slope V/dec	Cathode Tafel slope V/dec
without	-1.472	3.08×10^{-4}	0.049	0.248
sodium alginate	-1.300	4.45×10^{-5}	0.062	0.102
sodium silicate	-1.183	1.24×10^{-5}	0.078	0.084
SDBS	-1.232	2.56×10^{-5}	0.065	0.119

Figure 2 shows the corrosion inhibition efficiency of AM60B magnesium alloy in simulated vehicle coolant with different corrosion inhibitors. As can be seen from Figure 2, the corrosion inhibition efficiency is ranked from high to low as: sodium silicate>SDBS>sodium alginate. Meanwhile, sodium silicate has the highest corrosion inhibition efficiency and largest anode Tafel slope which is 96% and 0.078 V/dec respectively, confirming its best corrosion inhibition effect on AM60B magnesium alloy. The hydrolysis product of sodium silicate, such as magnesium silicate and magnesium hydroxide, which adsorb on the surface of magnesium alloy, may increase the membrane resistance resulting in higher anode Tafel slope.

When AM60B magnesium alloy is immersed in simulated vehicle coolant, a larger amount of hydrogen evolution and $Mg(OH)_2$ production covers the surface. With the increase of $Mg(OH)_2$ deposition, although a protective film can be formed, AM60B magnesium alloy is still continuously corroded due to its limited protection and corrosion inhibition because of its low density [28-29].

$$Mg-2e\rightarrow Mg^{2+} \quad (3)$$

$$2H_2O+2e\rightarrow 2OH^-+H_2\uparrow \quad (4)$$

$$Mg^{2+}+2OH^-\rightarrow Mg(OH)_2\downarrow \quad (5)$$

Sodium alginate is a kind of copolymer, which generates guluronic acid and mannuronic acid after hydrolysis, adsorbed on the surface of AM60B magnesium alloy to form a denser film layer through physical reaction. It can protect and inhibit corrosion process of AM60B magnesium alloy.

SiO_3^{2-} is generated after the hydrolysis of sodium silicate, which can react with Mg^{2+} to generate insoluble $MgSiO_3$ compound. The $MgSiO_3$ compound gradually deposits on the surface of

AM60B magnesium alloy to form a relatively dense film layer, playing a role of protection and corrosion inhibition. In addition, Mg^{2+} can react with OH^- to form $Mg(OH)_2$, which also has a certain inhibition effect.

$$Mg^{2+} + SiO_3^{2-} \rightarrow MgSiO_3 \downarrow \quad (6)$$

SDBS contains sulfonate polar groups and benzene alkyl non-polar groups, among which the sulfonate polar groups are hydrophobic, and are easily adsorbed on the surface of AM60B magnesium alloys to isolate the corrosive medium, thus playing a role in inhibiting the corrosion process of AM60B magnesium alloy. The corrosion inhibition effect of SDBS is also reported by some people [30-33]. In comparison, the reaction product of sodium silicate as a corrosion inhibitor deposits on the surface of AM60B magnesium to form a dense film layer, which can better isolate the corrosive ions and substances in simulated vehicle coolant to effectively inhibit the corrosion process of AM60B magnesium alloy.

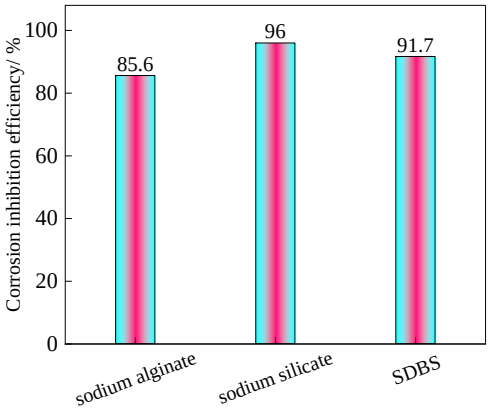

Figure 2. Corrosion inhibition efficiency of AM60B magnesium alloy in simulated vehicle coolant with and without corrosion inhibitors

3.2 Analysis of electrochemical impedance spectrum

Figure 3 shows the electrochemical impedance spectrum of AM60B magnesium alloy in simulated vehicle coolant without and with corrosion inhibitors. As can be seen from Figure 3, the electrochemical impedance spectrum of AM60B magnesium alloy shows similar characteristics in simulated vehicle coolant with and without corrosion inhibitors, both manifests as a capacitive reactance arc, approximately semi-circular. However, when sodium alginate, sodium silicate or SDBS is used as a corrosion inhibitor, the capacitive reactance arc radius of AM60B magnesium alloy is greater than without corrosion inhibitor, which further confirms that sodium alginate, sodium silicate or SDBS can play a corrosion inhibition role, so as to improve the corrosion resistance of AM60B magnesium alloy in simulated vehicle coolant.

Silicate could be used as corrosion inhibitor to reduce corrosion process extremely which is investigated in many works [34-36]. When sodium silicate is added as a corrosion inhibitor, the capacitive arc radius of AM60B magnesium alloy is the largest, and the corresponding charge transfer resistance is the highest, reaching 9.03×10^3 $\Omega\cdot cm^2$, as shown in Figure 4. The research shows that the

larger the radius of the capacitive reactance arc, the greater the resistance to the corrosion process. The higher the charge transfer resistance, the more difficult the electron transfer process at the two phase interface between the AM60B magnesium alloy and corrosive medium. Therefore, the corrosion inhibition effect of different corrosion inhibitors on AM60B magnesium alloy in simulated vehicle coolant is evaluated as follows: sodium silicate>SDBS>sodium alginate.

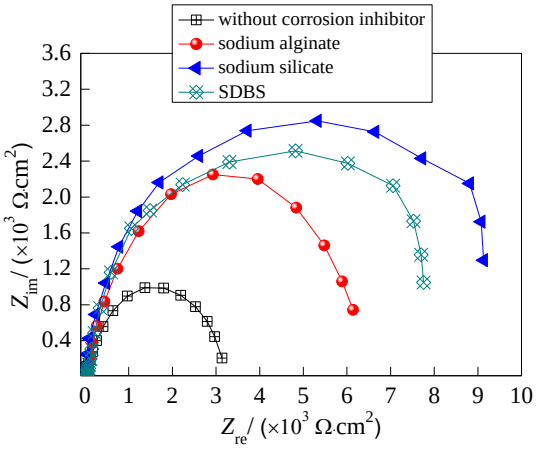

Figure 3. Electrochemical impedance spectrum of AM60B magnesium alloy in simulated vehicle coolant with and without corrosion inhibitors

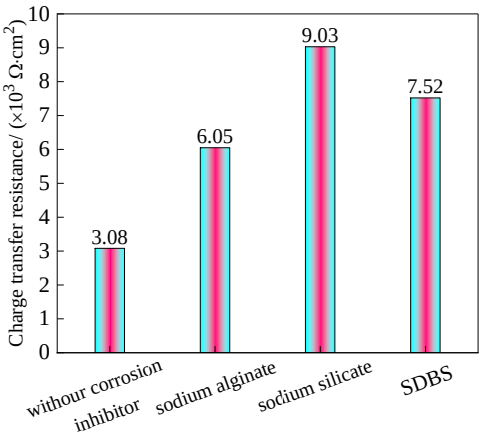

Figure 4. Analytical results of electrochemical impedance spectrum

3.3 Corrosion rate and corrosion morphology

Figure 5 shows the corrosion rate of AM60B magnesium alloy immersed in simulated vehicle coolant with and without corrosion inhibitors for different time. It can be seen from Figure 5 that with the prolongation of immersion time, the corrosion rate of AM60B magnesium alloy in simulated vehicle coolant with and without corrosion inhibitors all shows an increasing trend, indicating that the corrosion degree is gradually increasing. However, when immersed for the same time, the corrosion rate decreased significantly after adding different corrosion inhibitors. For example, when AM60B magnesium alloy is immersed in simulated vehicle coolant for 25 d, the corrosion rate without

corrosion inhibitor is 0.45 g/(m^2·d). However, after adding sodium alginate, sodium silicate or SDBS as corrosion inhibitor, the corrosion rate is 0.09 g/(m^2·d), 0.06 g/(m^2·d) and 0.08 g/(m^2·d), respectively. The lowest corrosion rate can indicate that sodium silicate has the best corrosion inhibition effect on AM60B magnesium alloy, which is better than that of sodium alginate and SDBS.

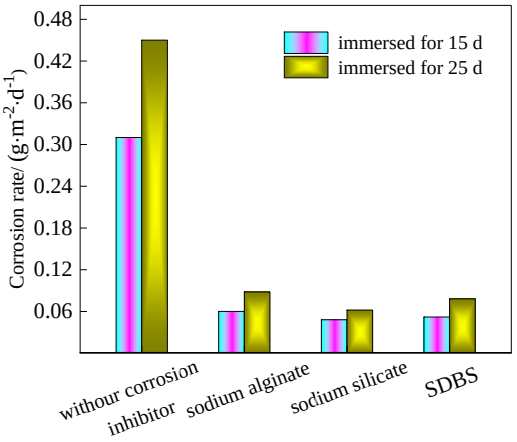

Figure 5. Corrosion rate of AM60B magnesium alloy immersed in simulated vehicle coolant with and without corrosion inhibitors for different time

Figure 6 and Figure 7 show the surface morphology and three-dimensional morphology of AM60B magnesium alloy immersed in simulated vehicle coolant with and without corrosion inhibitors for 25 d. The surface morphology of magnesium alloy immersed in vehicle coolant has been studied in related works [37-39]. Some of the surface morphology is different due to different compositions of vehicle coolant and different corrosion inhibitors. It can be seen from Figure 6 that a loose and porous film composed of corrosion products is formed on the surface of AM60B magnesium alloy, indicating that the corrosion degree of AM60B magnesium alloy is serious. When sodium alginate, sodium silicate or SDBS was added as corrosion inhibitors into simulated automobile coolant, the corrosion degree of AM60B magnesium alloy is obviously reduced, and a relatively uniform and dense corrosion products film is formed on the surface. Furthermore, when sodium silicate acts as a corrosion inhibitor, a flat and dense film composed of corrosion products is formed on the surface of AM60B magnesium alloy which possesses the least corrosion degree. The main reason is that the reaction products of sodium silicate with AM60B magnesium alloy is deposited on the surface to form a dense film layer, which can better isolate the corrosive ions and substances in the vehicle coolant, so as to protect AM60B magnesium alloy. The mechanism of sodium silicate as corrosion inhibitor is studied in many literatures [40-42].

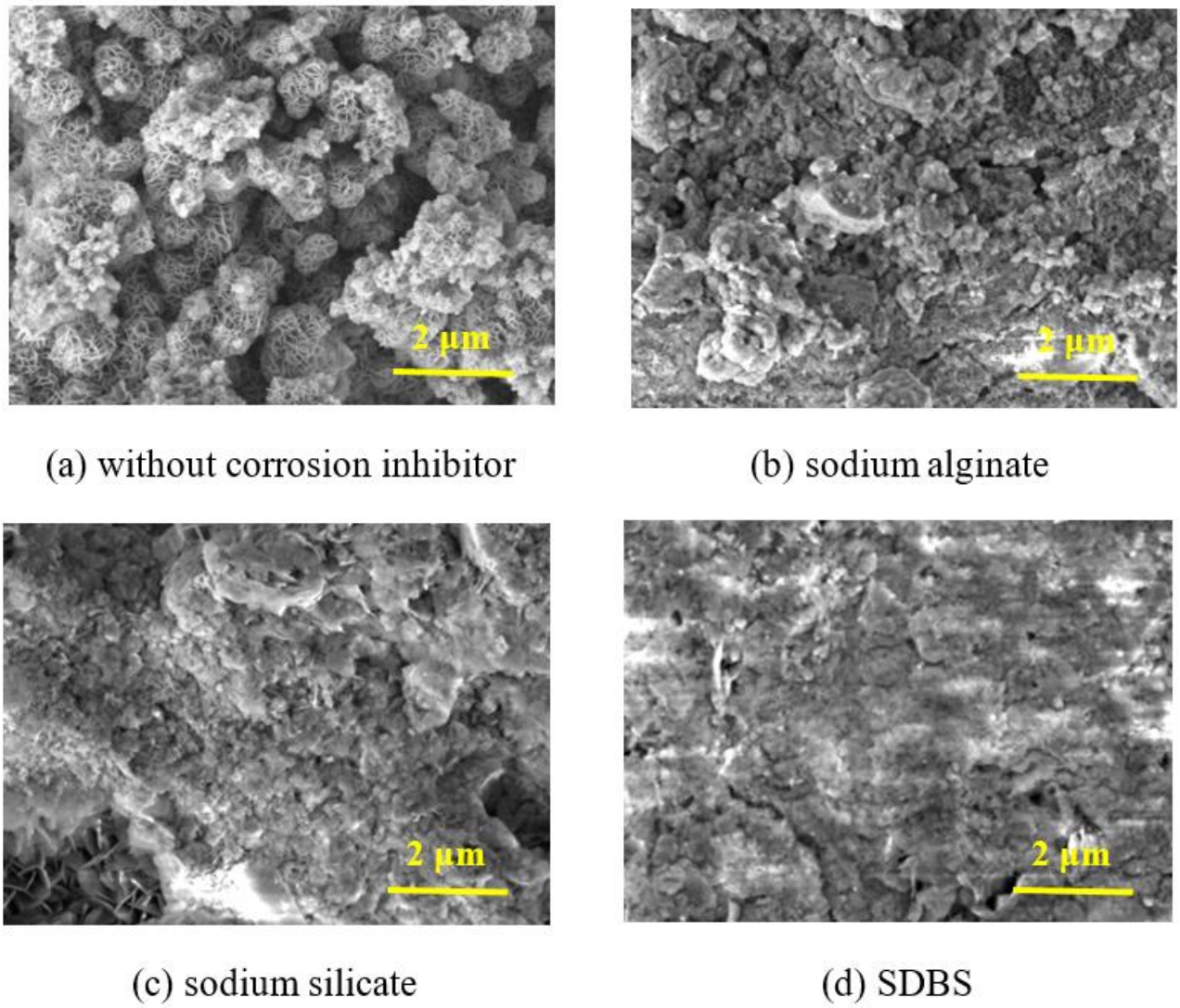

Figure 6. Surface morphology of AM60B magnesium alloy immersed in simulated vehicle coolant with and without corrosion inhibitors for 25 d

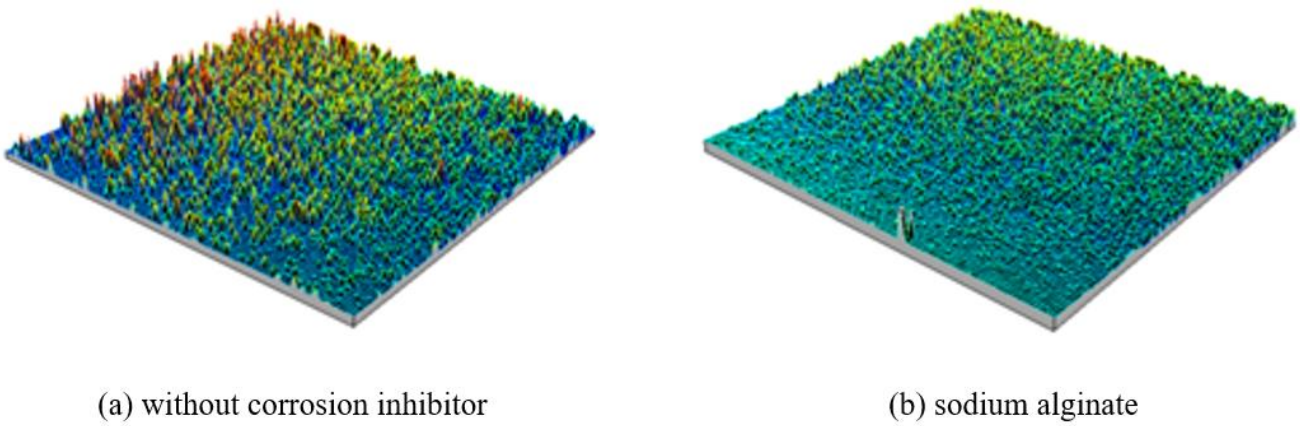

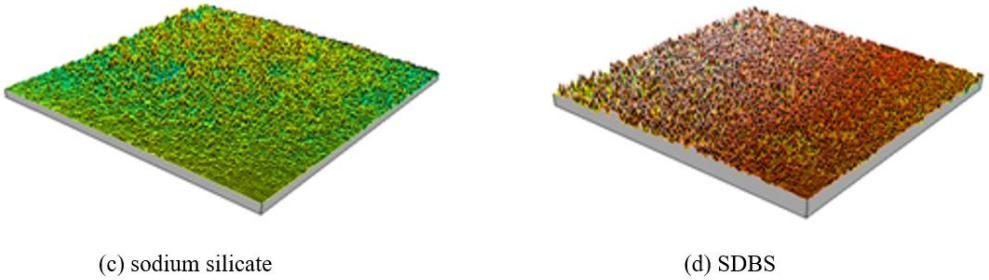

(c) sodium silicate (d) SDBS

Figure 7. Three-dimensional morphology of AM60B magnesium alloy immersed in simulated vehicle coolant with and without corrosion inhibitors for 25 d

4. CONCLUSIONS

Sodium alginate, sodium silicate and SDBS are selected as the corrosion inhibitors to inhibit the corrosion process of AM60B magnesium alloy in simulated vehicle coolant. The conclusions are as follows:

(1) Sodium alginate, sodium silicate or SDBS can inhibit the corrosion process of AM60B magnesium alloy in simulated vehicle coolant to reduce the corrosion rate and decrease the corrosion degree of AM60B magnesium alloy. Compared with sodium alginate and SDBS, the inhibition efficiency of sodium silicate for AM60B magnesium alloy is the highest, up to 96%, which is the best corrosion inhibitor.

(2) The reaction products of sodium silicate with AM60B magnesium alloy can better isolate the corrosive ions and substances in simulated vehicle coolant, and prevent further infiltration erosion, thus reducing the corrosion current density and corrosion rate of AM60B magnesium alloy, which play a better corrosion inhibition effect on AM60B magnesium alloy.

References

1. D. Kumar, R. K. Phanden and L. Thakur, *Mater. Today:. Proc.*, 38 (2021) 359.
2. J. D. Du, W. J. Han and Y. H. Peng, *J. Cleaner Prod.*, 18 (2010) 112.
3. S. V. S. Prasad, S. B. Prasad, K. Verma, R. K. Mishra, V. Kumar and S. Singh, *J. Magnesium Alloys*, 10 (2022) 1.
4. P. Umamaheswarrao, B. R. Sankar, M. Pardhasaradhi and K. Rajasekharababu, *Mater. Today:. Proc.*, 44 (2021) 305.
5. W. L. Yang, Z. Q. Liu and H. L. Huang, *Corros. Sci.*, 188 (2021) 109562.
6. L. B. Coelho, M. Lukaczynska-Anderson, S. Clerick, G. Buytaert, S. Lievens and H. A. Terryn, *Corros. Sci.*, 19 (2022) 110188.
7. X. Huang, L. T. Wang, Y. F. Song, F. Ge, Y. Zhang, X. J. Meng, H. H. Ge and Y. Z. Zhao, *J. Alloys Compd.*, 874 (2021) 159807.
8. S. Mukherjee, T. Halder, S. Ranjan, K. Bose, P. C. Mishra and S. Chakrabarty, *Energy*, 231 (2021) 120913.
9. X. K. Li, C. J. Zou and A. H. Qi, *Int. Commun. Heat Mass Transfer*, 77 (2016) 159.
10. Y. D. Yu, G. Y. Wei, L. Jiang and H. L. Ge, *Int. J. Electrochem. Sci.*, 15 (2020) 1108.
11. A. E. Somer, B. R. W. Hinton, C. D. B. Dickason, G. B. Deacon, P. C. Junk and M. Forsyth, *Corros. Sci.*, 15 (2018) 430.

12. Y. Peng, A. E. Hughes, G. B. Deacon, P. C. Junk, B. R. W. Hinton, M. Forsyth, J. I. Mardel and A. E. Somers, *Corros. Sci.*, 145 (2018) 199.
13. Y. H. Zhu, J. Zhuang, Y. S. Yu and X. G. Zeng, *J. Rare Earths*, 7 (2013) 734.
14. B. Davo and J. J. D. Damborenea, *Electrochim. Acta*, 49 (2004) 4957.
15. Y. H. Hu, Y. D. Yu, H. L. Ge, G. Y. Wei and L. Jiang, *Int. J. Electrochem. Sci.*, 14 (2019) 1649.
16. M. Javidi and R. Omidvar, *J. Mol. Liq.*, 291 (2019) 111330.
17. D. D. Li, F. Y. Wang, X. Yu, J. Wang, Q. Liu, P. P. Yang, Y. He, Y. L. Wang and M. L. Zhang, *Prog. Org. Coat.*, 71 (2011) 302.
18. F. Zhao, A. D. Liao, R. F. Zhang, S. F. Zhang, H. X. Wang, X. M. Shi, M. J. Li and X. M. He, *Trans. Nonferrous Met. Soc. China*, 20 (2010) 683.
19. Y. D. Yu, J. W. Lou, W. Li, L. X. Sun, H. L. Ge and G. Y. Wei, *Mater. Sci. Technol.*, 28 (2012) 448.
20. G. N. Mu, X. H. Li, Q. Qu and J. Zhou, *Corros. Sci.*, 48 (2006) 445.
21. M. B. Jensen, M. J. Peterson, N. Jadhav and V. J. Gelling, *Prog. Org. Coat.*, 77 (2014) 2116.
22. S. M. T. Takeuchi, D. S. Azambuja, A. M. Saliba-Silva and I. Costa, *Surf. Coat. Technol.*, 200 (2006) 6826.
23. K. A. Alghanab, D. Seifzadeh, Z. Rajabalizadeh and A. H. Yangjeh, *Surf. Coat. Technol.*, 397 (2020) 125979.
24. T. T. Hu, B. Xiang, S. G. Liao and W. Z. Huang, *Anti-Corros. Methods Mater.*, 57 (2010) 244.
25. Y. F. Liu, W. Yang, Q. L. Qin, Y. C. Wu, W. Wen, T. Zhai, B. Yu, D. Y. Li, A. Luo and G. L. Song, *Corros. Sci.*, 81 (2014) 65.
26. R. O. Hussein, D. O. Northwood and X. Nie, *J. Alloys Compd.*, 541 (2012) 41.
27. R. Samadianfard, D. Seifzadeh, A. H. Yangjeh and Y. J. Tarzanagh, *Surf. Coat. Technol.*, 385 (2020) 125400.
28. D. Merachtsaki, E. C. Tsardaka, E. Anastasiou and A. Zouboulis, Constr. *Build. Mater.*, 312 (2021) 125441.
29. Q. Jin, G. Y. Tian, J. X. Li, Y. Zhao and H. Yan, *Colloids Surf., A*, 577 (2019) 8.
30. H. Medhashree, and A. N. Shetty, *J. Adhes. Sci. Technol.*, 33 (2019) 523.
31. Y. J. Qiang, S. T. Zhang, L. Guo, S. Y. Xu, L. Feng, I. B. Obot and S. J. Chen, *J. Cleaner Prod.*, 152 (2017) 17.
32. S. S. Abdei-Rehim, M. A. Amin, S. O. Moussa and A. S. Ellithy, *Mater. Chem. Phys.*, 112 (2008) 898.
33. F. K. Kerkouche, A. Benchettara and S. Amara, *Mater. Chem. Phys.*, 110 (2008) 26.
34. B. Li, B. F. Trueman, M. S. Rahman and G. A. Gagnon, *J. Hazard. Mater.*, 407 (2021) 124707.
35. X. Liu, H. Q. He, T. C. Zhang, L. K. Ouyang, Y. X. Zhang and S. J. Yuan, *Chem. Eng. J.*, 404 (2021) 127106.
36. C. Wang, J. X. Chen, B. S. Hu, Z. Y. Liu, C. B. Wang, J. Han, M. Su, Y. H. Li and C. L. Li, *J. Cleaner Prod.*, 238 (2019) 117823.
37. W. Zhou, N. N. Aung, A. Choudhary and M. Kanouni, *Corros. Eng. Sci. Technol.*, 46 (2011) 386.
38. L. H. Han, X. Y. Nie and H. Hu, *Mater. Technol.*, 24 (2009) 170.
39. Z. W. Wang, W. Bai, Y. Yang, Y. Wu, C. W. Su and J. M. Guo, *Int. J. Electrochem. Sci.*, 11 (2016) 6110.
40. T. Y. Zheng, L. Wang, J. Y. Liu, J. Wang and G. X. Jia, *Colloids Surf., A*, 610 (2021) 125723.
41. H. Gao, Q. Li, F. N. Chen, Y. Dai, F. Luo and L. Q. Li, *Corros. Sci.*, 53 (2011) 1401.
42. R. U. Din, K. Bordo, N. Tabrizian, M. S. Jellesen and R. Ambat, *Appl. Surf. Sci.*, 423 (2017) 78.